

Supplementary Material

Blue photoluminescence of wide-bandgap polystyrenesulfonate materials

Wenqian Zhang^{1†}, Lu Wan^{1†}, Dehua Yang^{1,2*}, Jianxin Guo¹, Xin Zhou¹, Xiaoyang Yuan¹,
Xuan Chang¹, Cuili Zhang¹, Jianhui Chen^{1,2*}

*Address correspondence to: chenjianhui@hbu.edu.cn, yangdehua@hbu.edu.cn.

†These authors contributed equally to this work.

¹*Advanced Passivation Technology Lab, College of Physics Science and Technology, Hebei University, Baoding 071002, China.*

²*State Key Laboratory of Photovoltaic Materials and Cells, Yingli Group Co., Ltd, Baoding 071051, China.*

E-mail: chenjianhui@hbu.edu.cn , yangdehua@hbu.edu.cn.

1. Experimental Section

Preparation of solution: The PSS solution is an 18 wt% aqueous solution (Sigma manufacturer). The PSS solution was diluted by adding different volumes of deionized water to form a solution of 0 wt% to 18 wt% by mass (as shown in Table 1). Simple magnetic stirring for at least 6 hours was used to obtain a homogeneous solution. The pH of the PSS solution was varied by adding different volumes of KOH (Sigma manufacturer). The strength of the applied magnetic field is changed by placing a magnet near the solution during the fluorescence spectrophotometer test.

Optical measurements: Solution absorption spectra were measured using a PerkinElmer Lambda 950 UV-Vis spectrophotometer device. Solution PL spectra were tested using a fluorescence spectrophotometer (F-7100). PH value measurement: Lichen pH-100Pro. Magnetic field strength test: Gauss meter, AIKESI GS-25. Film thickness test: probe surface profiler (Bruke-Dektak XT). The path of the optical cuvette used for PL spectra measurements is shown in Fig. S5.

2. Relative fluorescence quantum yields of PSS at different concentrations

Fluorescence quantum yield ($\Phi(f)$)¹⁻³ is a key parameter for evaluating the luminescent properties of fluorophores. $\Phi(f)$ can be defined as the ratio of the number of photons emitted by a luminescent material to the number of photons absorbed, which is a direct measure of the efficiency with which absorbed light is converted into emitted light. The $\Phi(f)$ of transparent samples (e.g., molecular fluorophore solutions, most fluorophore-labeled biomolecules, and small-sized quantum dots) can be determined optically based on a fluorescence standard with a known $\Phi(f)$. The most widely used relative optical method relies on comparing the integral emission spectrum of a sample with the resulting standard of a solution with a known absorption coefficient of absorbance or excitation wavelength under identical measurement conditions. Fig. 3(b) shows the relative $\Phi(f)$ of PSS solutions at 0-5 wt% concentration relative to 0.05 wt% concentration. Establishing the quantitative relationship between the relative $\Phi(f)$ of PSS and concentration is important for the study of the performance and photoluminescence mechanisms of PSS. Therefore, based on the changes in the intensity of absorption and emission spectra of PSS solutions at different concentrations, we further quantified the changes in the relative $\Phi(f)$ of PSS solutions with concentration. The specific transmission path of the excitation/emission light is a right-angle path, as shown in Fig. S5. The fluorescence quantum yield $\Phi(x\%)$ of PSS solutions with different concentrations (x%) for any volume element (dx dy dz) can be expressed as

$$\Phi(x\%) = \frac{I_{(x\%)}}{2.3 \frac{\Omega}{4\pi} I_0 \varepsilon_{(PSS)} k A_{(360nm)} \iiint 10^{-A_{(360nm)}y} 10^{-A_{(465nm)}x} dx dy dz} \quad (1)$$

Different concentrations of PSS solution relative to the concentration of 0.05 wt% relative fluorescence $\Phi(x\%)/\Phi(0.05\%)$ can be expressed as

$$\frac{\Phi_{(x\%)}}{\Phi_{(0.05\%)}} = \frac{I_{(x\%)} A_{(360nm)} \iiint 10^{-A_{(360nm,0.05\%)}y} 10^{-A_{(465nm,0.05\%)}x} dx dy dz}{I_{(0.05\%)} A_{(360nm)} \iiint 10^{-A_{(360nm,x\%)}y} 10^{-A_{(465nm,x\%)}x} dx dy dz} \quad (2)$$

Where $\Phi_{(x\%)}$ is the PL quantum yield of PSS whose mass fraction is $x\%$; $I_{(x\%)}$ is the emission intensity of PSS with a mass fraction of $x\%$; $\frac{\Omega}{4\pi}$ is the ensemble solid Angle of the detector; I_0 is the original intensity of incident light per unit area before entering the solution; $\epsilon_{(PSS)}$ is the molar absorption coefficient of PSS at a specific excitation wavelength; $A_{(360nm)}$ is the absorbance of PSS solution at the excitation wavelength of 360nm. Since the absorbance of $A_{(360nm)}$ of PSS is directly proportional to the relative concentration, as shown in Fig. 3a, concentration c and absorbance $A_{(360nm)}$ can be expressed as $c = kA_{(360nm)}$. The y and x are excitation directions and detection directions, respectively. The dimensions of c and l are $\text{mol}\cdot\text{cm}^{-3}$ and cm , respectively.

3. Effect of pH on PL intensity of PSS

Based on the above experimental results, we have hypothesised that the luminescent properties of PSS solutions depend on the concentration of hydrogen ions in the solution. The initial PSS solution is acidic, which is due to the partial dissociation of the protons of the molecules in solution.⁴ The proton dissociation process is reversible, and when a small amount of KOH solution is added to the solution, OH^- reacts with the partially ionized H^+ in a neutralization reaction, promoting the positive dissociation process. As the amount of KOH added increases, the relative number of dissociated protons on the sulfonic acid group tends to saturate, and ultimately, when the solution becomes neutral or basic, the proton dissociation process of PSS is inhibited, and the hydrogen ions in the solution are essentially neutralised, resulting in the loss of luminescent properties of the PSS solution.

4. Effect of magnetic field intensity on PL intensity of PSS

In academic studies in the 1960s and 1970s, it was observed that low magnetic fields (less than 500 mT) can significantly affect electroluminescence, PL, photocurrent, and electrically injected currents in nonmagnetic organic semiconductor materials, which in turn induces MFEs.^{5, 6} Quantum statistical analyses indicate that in organic materials, the spin polarization of electrons and holes leads to a 1:3 ratio between singlet and triplet states. Typically, the proportion of spin

triplet excited states is about 75%, while spin singlet states account for 25% of the total number of excited states.^{6, 7} In intermolecular excited states, the magnetic field-dependent single- to triple-heavy-state ratio can be tuned in three ways: spin-dependent formation process, deviation of the Lund g-factor, and field-sensitive intersystem crossing (Intersystem Crossing, ISC).^{8, 9} However, both experimental and theoretical studies have shown that low magnetic fields do not significantly affect the spin-polarization effect in non-magnetic semiconductor materials. The Lund g-factor deviation mechanism is only effective in strong magnetic field environments (magnetic field strength greater than 1 Tesla). The third mechanism involves the exogenous-Zeeman splitting induced by the applied magnetic field on the excited states of the triplet intermolecular states. If the outer Zeeman splitting is larger than the inner Zeeman splitting, it is possible to alter the ISC process. Thus, ISC affected by magnetic field changes becomes an effective mechanism to regulate the ratio of singlet to triplet states in the intermolecular excited states under photoexcitation.

For the ISC of intermolecular excited states, external Zeeman splitting may lead to two different results. In states where the electron-hole (e-h) separation distance is small, the singlet-triplet state energy difference caused by spin-exchange interactions is much larger than the Zeeman splitting. The applied magnetic field reduces the energy gap between the singlet and triplet states. When ISC is a phonon-assisted leap from Tm1 to S, decreasing the energy gap favors the ISC process and thus increases the proportion of single heavy states. Thus, magnetic field-dependent ISC enhances the PL intensity, leading to a positive magnetic field effect in the intermolecular excited states, especially when the electron-hole separation distance is short. On the contrary, when the electron-hole separation distance is large, the increasing exogenous-Zeeman splitting may lead to the intersection of single-linear and triplet state energy levels and the formation of a flat crossing point. As a result, the ISC process shows a non-monotonic trend of increasing and then decreasing, and the MFEs first show positive and then turn negative with the increasing magnetic field before and after the flat crossing point. In this study, the experimental data pointed out that the magnetic field-dependent ISC could enhance the PL intensity, leading to a positive magnetic field effect in the intermolecular excited state, and the PL intensity was continuously enhanced with the increase of the magnetic field intensity. In

addition to this, it was found that the external magnetic field has no effect on the peak position of the PSS luminescence intensity, showing essentially the same characteristics.

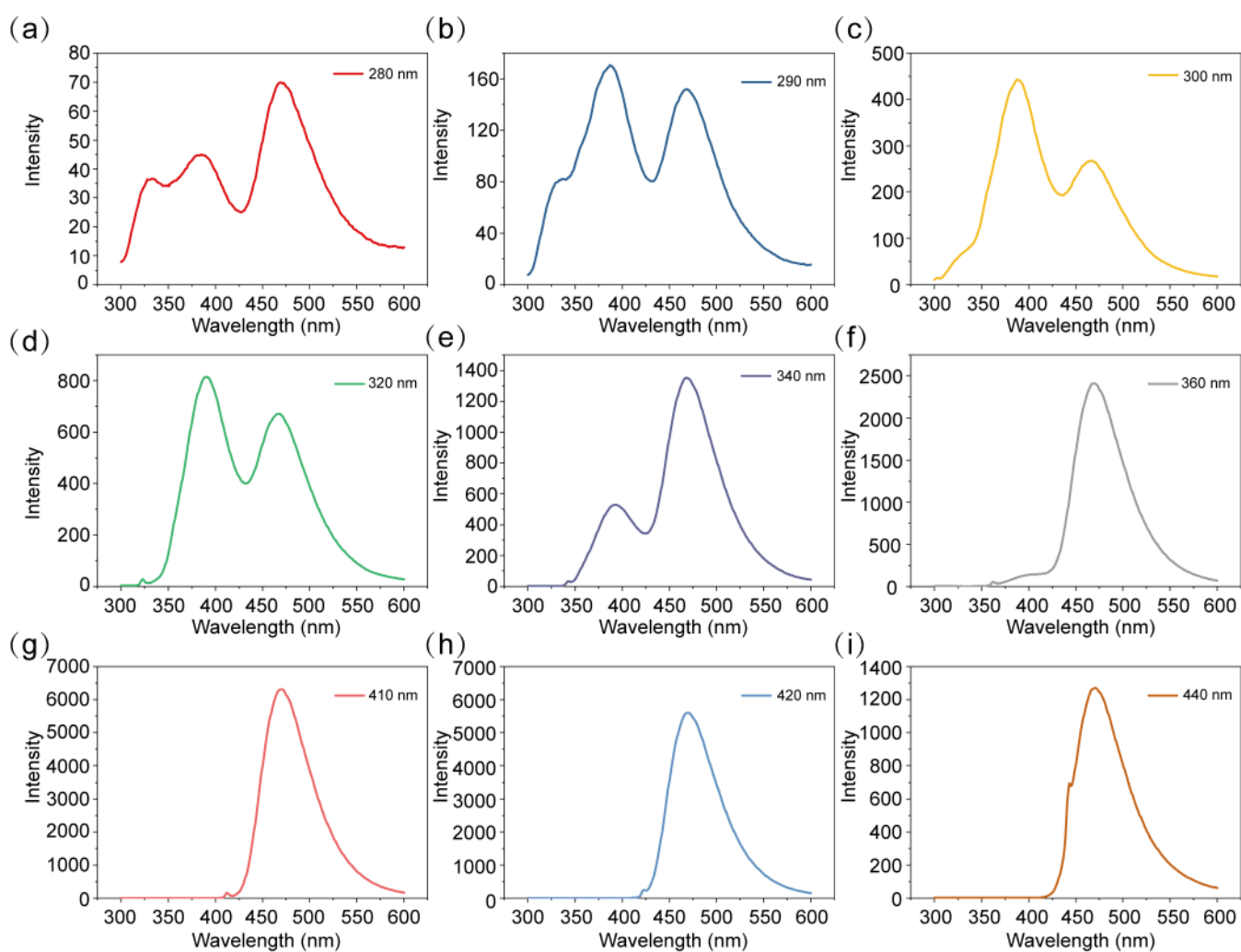


Fig. S1, (a)-(i) The emission spectra of PSS solutions were obtained at different excitation wavelengths. The emission peaks decrease gradually from three at 330 nm, 384 nm, and 469 nm, and finally only one emission peak is retained at 469 nm.

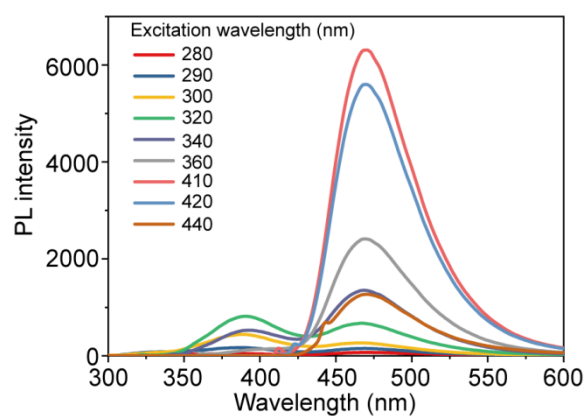


Fig. S2, Summary of emission spectra of PSS solutions obtained at different excitation wavelengths.

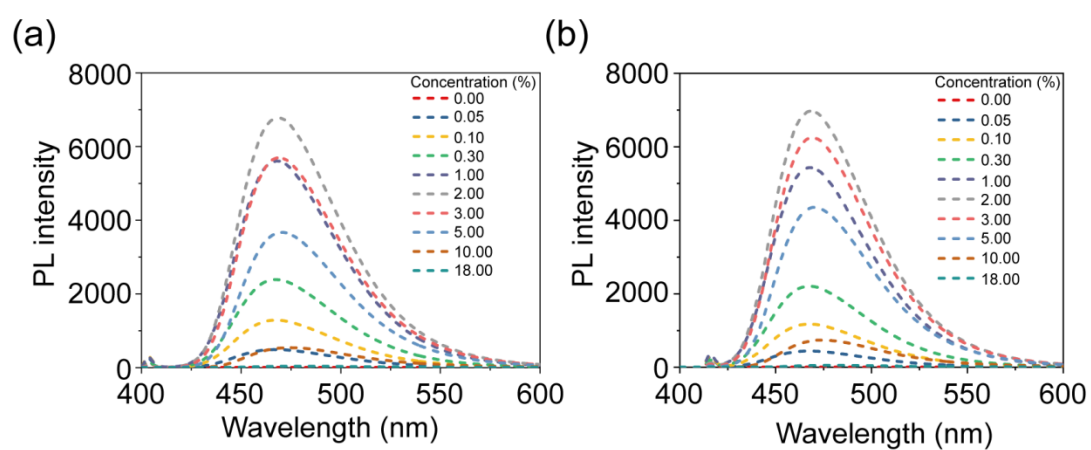


Fig. S3, Emission spectra of 0wt% ~ 18wt% PSS solutions at (a) 402 nm and (b) 414 nm excitation wavelengths.

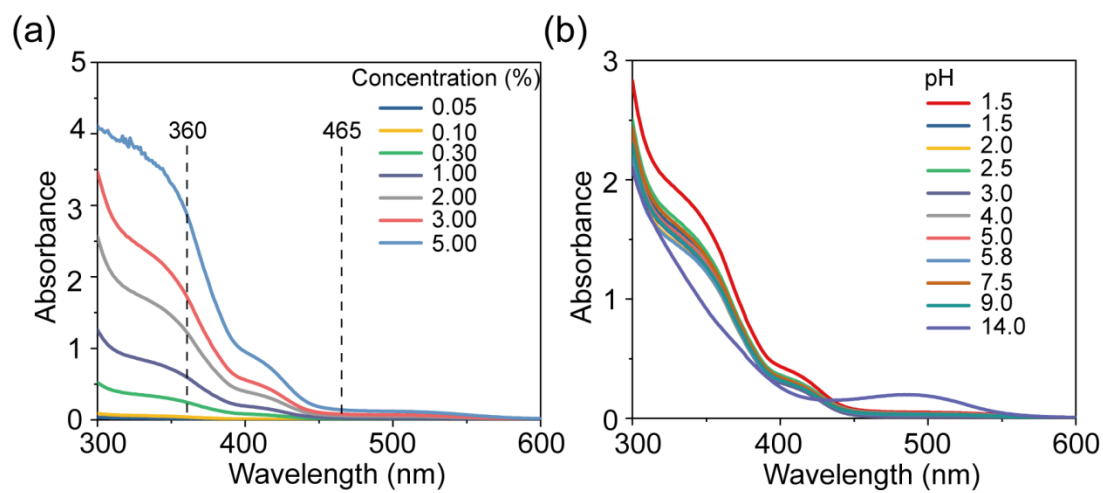


Fig. S4, (a) Absorption spectra of 0 wt%–5 wt% PSS solutions. (b) Absorption spectra of 2 wt% PSS solutions at different pH values.

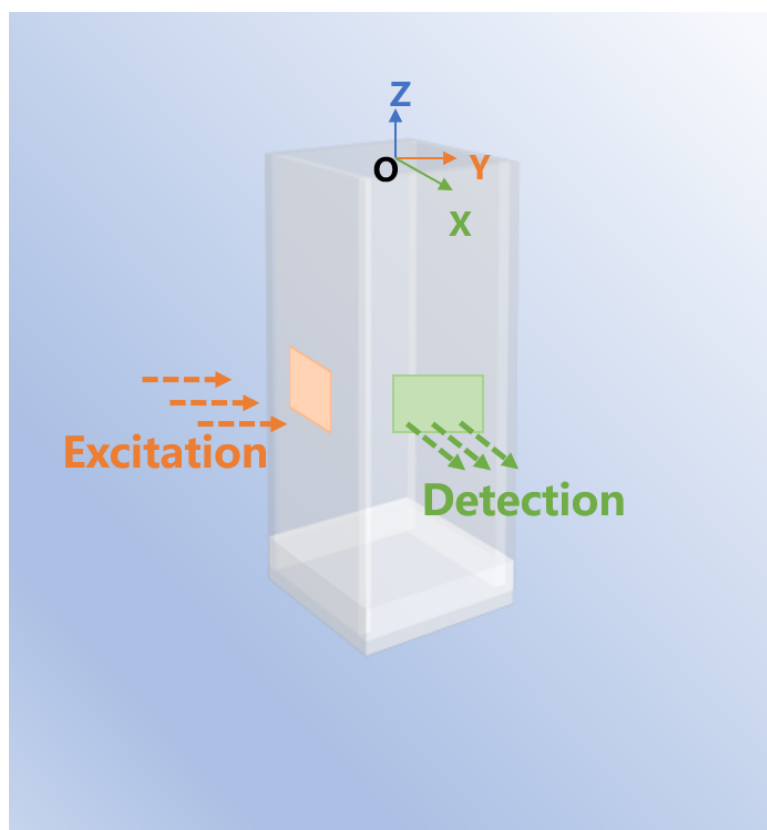


Fig. S5, Schematic diagram of the cuvette for PL spectra measurement with an angle of 90° between the excitation and detection directions.

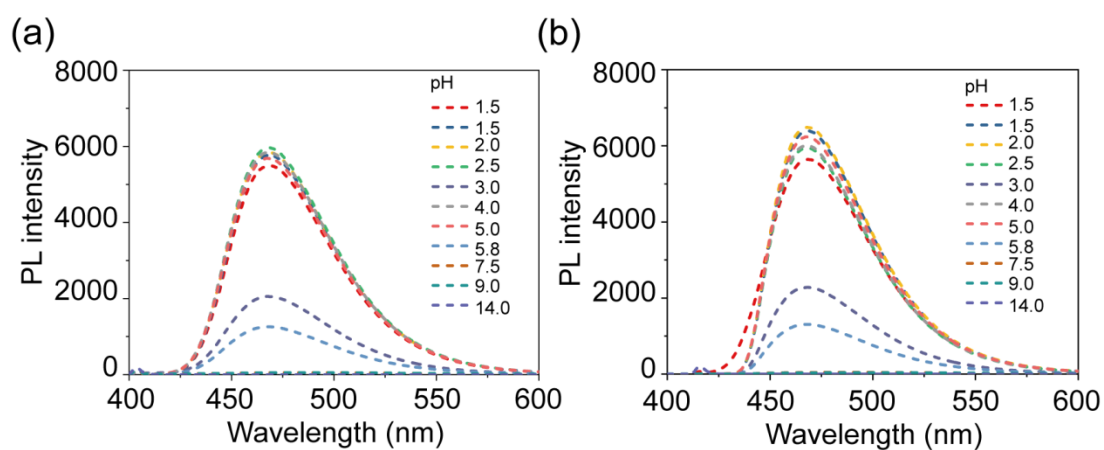


Fig. S6, Emission spectra of 2 wt% PSS solutions at different pH values at (a) 402 nm and (b) 414 nm excitation wavelengths.

References

1. T. O. Pereira, M. Warzecha, L. H. C. Andrade, J. R. Silva, M. L. Baesso, C. J. McHugh, J. Calvo-Castro and S. M. Lima, *Phys Chem Chem Phys.*, 2020, **22**, 25156-25164.
2. C. Würth, M. Grabolle, J. Pauli, M. Spieles and U. Resch-Genger, *Nat Protoc.*, 2013, **8**, 1535-1550.
3. B. Hu, L. Yan and M. Shao, *Adv. Mater.*, 2009, **21**, 1500-1516.
4. O. P. Dimitriev, Y. P. Piryatinski and A. A. Pud, *J Phys Chem B.*, 2011, **115**, 1357-1362.
5. V. Ern and R. E. Merrifield, *Phys Rev Lett.*, 1968, **21**, 609-611.
6. H. J. Werner, Z. Schulten and K. Schulten, *J Chem Phys.*, 1977, **67**, 646-663.
7. G. Vazquez, C. Camara, S. J. Putterman and K. Weninger, *Phys Rev Lett.*, 2002, **88**, 197402.
8. T. J. Penfold, E. Gindensperger, C. Daniel and C. M. Marian, *Chem Rev.*, 2018, **118**, 6975-7025.
9. H. T. Z. Zhu, I. Badía-Domínguez, B. B. Shi, Q. Li, P. F. Wei, H. Xing, M. C. R. Delgado and F. H. Huang, *J Am Chem Soc.*, 2021, **143**, 2164-2169.